Bio-Design and Manufacturing (2024) 7:453–462
https://doi.org/10.1007/s42242-024-00290-6

RESEARCH ARTICLE

Soft, body conformable electronics for thermoregulation enabled by kirigami

Lung Chow[1] · Guangyao Zhao[1] · Pengcheng Wu[1] · Xingcan Huang[1] · Jiyu Li[1,2] · Jian Li[1,2] · Wanying Wang[3] · Guihuan Guo[1] · Zhiyuan Li[1] · Jiachen Wang[1] · Jingkun Zhou[1,2] · Yawen Yang[1] · Yuyu Gao[1] · Binbin Zhang[1,2] · Qiang Zhang[1] · Dengfeng Li[1,2] · Ya Huang[1,2] · Kuanming Yao[1] · Jian Lu[4] · Xinge Yu[1,2]

Received: 26 September 2023 / Accepted: 5 May 2024 / Published online: 12 July 2024

Abstract

The application of thermoelectric devices (TEDs) for personalized thermoregulation is attractive for saving energy while balancing the quality of life. TEDs that directly attach to human skin remarkably minimized the energy wasted for cooling the entire environment. However, facing the extreme dynamic geometry change and strain of human skin, conventional TEDs cannot align with the contour of our bodies for the best thermoregulation effect. Hence, we designed a kirigami-based wearable TED with excellent water vapor permeability, flexibility, and conformability. Numerical analysis and experimental results reveal that our product can withstand various types of large mechanical deformation without circuit rupture. The stated outcome and proposed facile approach not only reinforce the development of wearable TEDs but also offer an innovative opportunity for different electronics that require high conformability.

Lung Chow, Guangyao Zhao, and Pengcheng Wu have contributed equally to this work.

✉ Jian Lu
jianlu@cityu.edu.hk

✉ Xinge Yu
xingeyu@cityu.edu.hk

[1] Department of Biomedical Engineering, City University of Hong Kong, Hong Kong 999077, China

[2] Hong Kong Centre for Cerebro-Cardiovascular Health Engineering, Hong Kong 999077, China

[3] Department of Biomedical Sciences, City University of Hong Kong, Hong Kong 999077, China

[4] Department of Mechanical Engineering, City University of Hong Kong, Hong Kong 999077, China

Graphic abstract

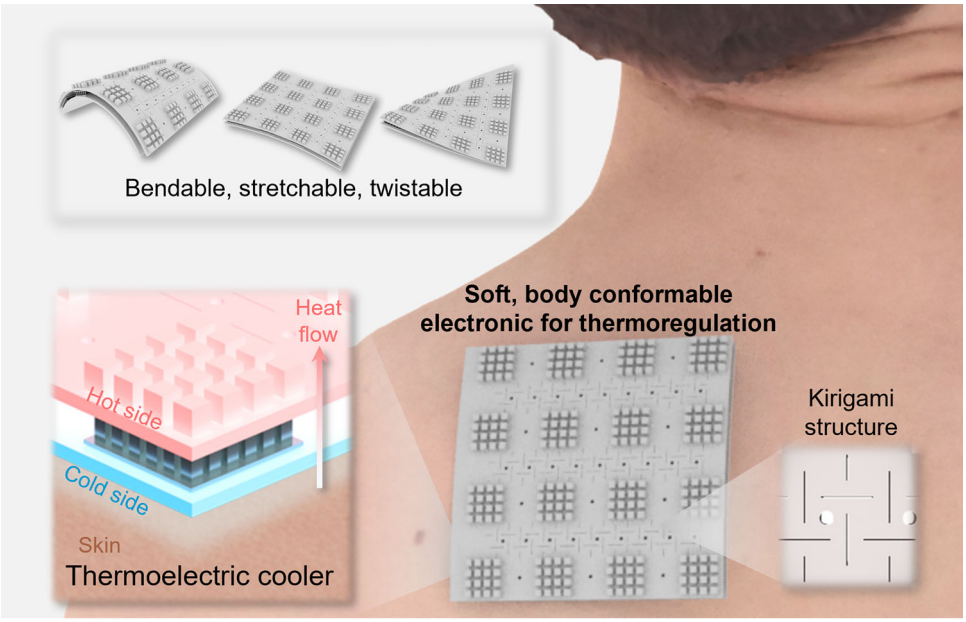

Keywords Thermoregulation · Thermoelectric · Kirigami · Body conformable · Wearable

Introduction

Thermoregulation of the body plays important roles in human health, life quality, productivity, and economics [1–3]. Owing to the limited ability of self-thermal regulation of the human body (core temperature needs to be maintained at (37±0.5) °C to ensure the appropriate function of metabolic processes [4]), we mostly rely on equipment, i.e., centralized climate control systems, to create an appropriate indoor temperature [5]. The estimated global energy used for air conditioning will increase from 2020 terawatt hours (TWh) in 2016 to 6200 TWh in 2050 [6]. The dramatic increase in energy consumption results in substantial CO_2 emissions associated with the fossil fuels used for power generation [7, 8]. Hence, developing new technologies to improve energy efficiency or improve the application is significant. Recently, wearable thermal regulation technologies, which will only change the localized temperature without changing the ambient temperature, have garnered attention [9–15]. This localized thermal management strategy not only conserves energy but also offers personalized comfort, allowing individuals to customize their thermal experience.

Among the various types of wearable temperature regulation devices, the thermoelectric devices (TEDs) which convert electricity into heat flux from one side to the other exhibit great advantages [16–18]. The working process of TEDs does not associate with chemical reactions, moving components, and working fluids and emits zero carbon [19, 20]. Conventional high-performance TEDs are usually based on inorganic rigid materials, which are not capable of conforming to the complex geometry of the human body. The key to realizing good thermoregulation by wearable TEDs is by forming perfect contact between the device and skin [21–23]. Therefore, various strategies have been reported for realizing flexibility and stretchability of TEDs or electronics [24, 25]. For instance, high conductive or heat capacity materials, such as aluminum nitrate (AlN), graphite, and paraffin, have been added to soft elastomers as the outermost layer of various devices [2, 26–30]. Moreover, the concepts of origami have been utilized to provide flexibility to devices by enabling self-folding [31, 32]. When considering origami, kirigami, as a variation of origami, allows the practitioner to exploit cuts along with folds to achieve large deformations in a relatively facile manner [33]. Kirigami technique has been exploited to design various types of highly stretchable devices [34–36]. However, incorporating kirigami patterns into TEDs for thermoregulation to obtain conformability to the human body contours is still not mature.

In this study, we report a strategy to realize flexible and stretchable TEDs with good air permeability for wearable thermoregulation by incorporating the kirigami concept for wearable conformability improvement. The combination of kirigami pattern and well-established stretchable circuit [37–42] ensures a large degree of deformation of the device without performance loss. The openings created by the kirigami pattern enable water vapor transmissibility to

ensure skin comfort. Computational analysis of the proposed design enables the wearable TED to exhibit good mechanical properties. The device can withstand 0.2 tensile strain and 60° of twisting, and has a 30-mm bending radius without circuit breakage. The results suggest that the proposed device is capable of achieving a cooling effect of 3.5 °C on the human skin. These results suggest that the wearable TED can not only be limited to thermoregulation applications, but also be applied to health-related uses, such as thermal therapy and wound care. The endeavor to incorporate kirigami patterns through facile manufacturing methods to enhance conformability to the human body is not restricted to TEDs and could potentially be employed in various soft wearable electronics.

Materials and methods

Fabrication of AlN/silicone gel and assembly method of TEDs

AlN power (about 1-μm diameter, purchased from Macklin, China) was first thoroughly mixed with silicone gel (Ecoflex™ 00-30, Smooth-On, Inc., USA) using a pestle and mortar for 10 min. Then, the mixture was poured into a mold and vacuum-degassed for curing. On the top layer AlN/silicone gel (with heatsink pillar), a laser cut polyimide/copper (PI/Cu) thin film (20 μm) stretchable serpentine circuit was attached on the uncured gel. After the AlN/silicone gel was fully cured (10 h at room temperature), it was removed from the mold and subjected to a laser cutting process by a desktop fiber laser marking machine (DMF-B-A, GD Han's Yueming Laser Group Co., Ltd., China). The wavelength of the laser emitted from the machine was approximately 1064 nm. Then, the gel was cleaned with acetone (a regular solvent for silicone gel cleaning [43]), to remove the dark residual created by the laser cutting process, and left at room temperature for 24 h before further fabrication. Finally, a 4×4 thermoelectric Peltier (Model number: OT016086, Shenzhen Tecooler Technology Co., Ltd., China; size: 10.00 mm × 10.00 mm × 1.95 mm) array was affixed with the same ratio of AlN/silicone mixture as adhesive agent on both sides and soldered on the serpentine circuit.

Characterizations

The tensile properties of PI/Cu film and different ratios of AlN silicone gel were characterized as per ASTM D638-14 Standard Test Method for Tensile Properties of Plastics (Type V specimen) at a speed of 100 mm/min using the Instron 5566 universal mechanical test frame. During the tensile test, images were captured at every 0.05 increase in axial strain. The changes in the axial (Δl) and lateral (Δl_{L}) lengths were examined through image analyses. The axial strain (ε) and lateral strain (ε_{L}) are obtained by using the following equations:

$$\varepsilon = \frac{\Delta l}{l}, \tag{1}$$

$$\varepsilon_{\mathrm{L}} = \frac{\Delta l_{\mathrm{L}}}{l_{\mathrm{L}}}, \tag{2}$$

where l and l_{L} denote the axial length and lateral length of the samples, respectively.

Poisson's ratio (υ) of the samples is calculated using

$$\upsilon = -\frac{\varepsilon_{\mathrm{L}}}{\varepsilon}. \tag{3}$$

The thermal conductivity (k) of the silicone gel with different AlN particle ratios was evaluated using TCi thermal conductivity analyzer (C-Therm, Canada), as per ASTM D5930-17 Standard Test Method for thermal conductivity of plastics by means of a transient line-source technique. The adhesion between the silicone gel and thermoelectric Peltier was tested in accordance with ASTM D5169 [44] at a speed of 305 mm/min. The rheological behavior of the uncured silicone gel with different AlN particle ratios was evaluated by a rheometer (Kinexus Pro+, Netzsch, Germany) with a cone-plate (radius: 40 mm; cone angle: 1.985°), and the truncation gap was 1 mm. The strain for frequency sweep was fixed at 1%, and the experiment was controlled at 25 °C. The standard test methods for water vapor transmission of materials, ASTM E96, were referenced to measure the water vapor transmission rate. The scanning electron microscope (SEM) images of the cross-sectional view of AlN/silicone gel were obtained using FEI Quanta 250. The electric resistance of the device was measured using the Keithley 2400 SourceMeter. The cooling or heating performance of the wearable TED was characterized by the setup shown in Fig. S1 (Supplementary Information). The temperature of the heater was set to be 32°C . Four thermocouples were used to record the temperature differences across the entire TED. CHI 660E electrochemical workstation was used to measure the electric performance of the TED. The current densities were calculated by dividing the current by the thermoelectric Peltier area (16 cm^2), whereas power densities were calculated by multiplying current densities and potentials.

Numerical analysis

The numerical analysis of the mechanical deformation of the wearable TED was performed using finite element analysis. The three-dimensional (3D) models of the devices were built in SolidWorks 2022 and meshed using MSC Apex 2020. The mesh files were imported into MSC Marc/Mentat software

for simulation. Friction was neglected in the finite element analysis. Based on the strain energy function shown below, the tensile test result was fitted to the third-order deformation model:

$$W = C_{10}(I_1 - 3) + C_{01}(I_1 - 3) + C_{11}(I_1 - 3)(I_2 - 3) + C_{20}(I_1 - 3)^2 + C_{30}(I_1 - 3)^2, \quad (4)$$

where W denotes the deviatoric third-order deformation strain energy function; C_{10}, C_{01}, C_{11}, C_{20}, and C_{30} are the material constants in the tensile test; and I_1 and I_2 are the initial two invariants of the strain tensor. Table S1 (Supplementary Information) contains the description of the materials and mesh properties.

Wear trial

A 23-year-old male subject was recruited for the trial of the wearable TED. An infrared camera (FLIR ONE®, Teledyne FLIR, USA) was used to capture the infrared image. The subject was requested to first put on the wearable TED on the forearm for 10 min to stabilize the skin and TED temperatures. Next, electricity (0.50 A for cooling and −0.25 A for heating) was applied to the TED for 20 min. The infrared image was captured once the TED was removed after 20 min of heating or cooling. The subject had a 30-min resting period after the removal of TED before the next cycle of experiment for stabilizing the body thermoregulation system, which was interrupted by the heating or cooling effect of the TED.

Results and discussion

Design and fabrication of wearable TEDs

Figures 1a–1c show the concept and design of the body-conforming kirigami wearable TED that can be fabricated using well-established technologies in an extremely facile manner. A 4×4 small-size commercial thermoelectric Peltier (10.00 mm×10.00 mm×1.95 mm) array was sandwiched between two layers of high thermal conductivity silicone gels (AlN/silicone gel) (Fig. 1b). The conformability and thermoregulation effect of the wearable TED can be affected by the thickness of the AlN/silicone gel. Although thinner gel layers can increase the conformability of the device, its application may not be as durable. A 1-mm-thick silicone gel was implemented to prevent easy gel tearing to achieve a compromise between performance and practicality. The thermoelectric Peltier array was connected by a stretchable serpentine circuit, as illustrated in Fig. S2 (Supplementary Information). Moreover, further reducing the thickness of thermoelectric Peltier can cause distinctive reduction in the temperature difference effect [2]. On the top of each thermoelectric Peltier, a 4×4 flexible heatsink pillar (1.75 mm× 2.00 mm) array was designed on the outermost layer of silicone gel to facilitate heat dissipation (Fig. 1c). Unlike the conventional rigid metal heatsinks that are applied in TED design, it prevents the human body from potential risks. Moreover, the implementation of the heatsink structure increases the surface area by about 3.3 times, allowing for easier heat exchange with the surrounding air. An inadequate heat exchange rate could compromise the cooling capabilities of TEDs. Body conformability is the key factor affecting the thermal regulating effect of TEDs in real situations. Therefore, the auxetic kirigami structure (rotating square) was designed between the thermoelectric Peltiers for the top and bottom layers of silicone gels to further elevate the wearability of the device (Fig. 1c). The rotating square shows relatively small out-of-plane deformation under stretching unlike other types of kirigami structures, such as folding wall, and can seriously affect the contact between the device and human body [45–47]. The unique auxetic property can improve the shape formability of the device, especially on a synclastic curvature surface, which is often seen on the human body [46, 48]. The laser cutting technique was utilized to create the intended kirigami structures [41, 49]. Owing to the narrow focal spot (radius: 0.00725 mm), a high-definition pattern can be carved with minimal impact on the surrounding area.

The thickness of the device was controlled to be around 5 mm to ensure conformability. The fabrication process and required materials are relatively facile, thus requiring less equipment (Fig. S3 in Supplementary Information). The laser cutting process can be completed by a fiber laser desktop machine within 30 s.

Mechanical simulation

The structural design of the device was subjected to finite element analysis to evaluate its mechanical performance. The experimental tensile test data of PI/Cu film and the AlN/silicone gel were input into the finite element model for calculation. Figures 2a–2f show the comparison between the experimental and simulation results of the device under stretching (strain: 0.2), twisting (twist angle: 60°), and bending (bending radius: 30 mm). Based on the simulation results, the strain of the electrical circuit under the abovementioned mechanical conditions is within 3%, which is the breaking strain of the used PI/Cu thin film (Fig. 2g). During the tensile experiments of AlN/silicone gel for curve fitting in the finite element model, we observed that Young's modulus increases by 8% when the AlN content increases from 0% to 37.5% (Fig. 2h). We also conducted a bending test based on the finite element analysis to quantify the conformability of the designed kirigami structure. The schematic of simulations

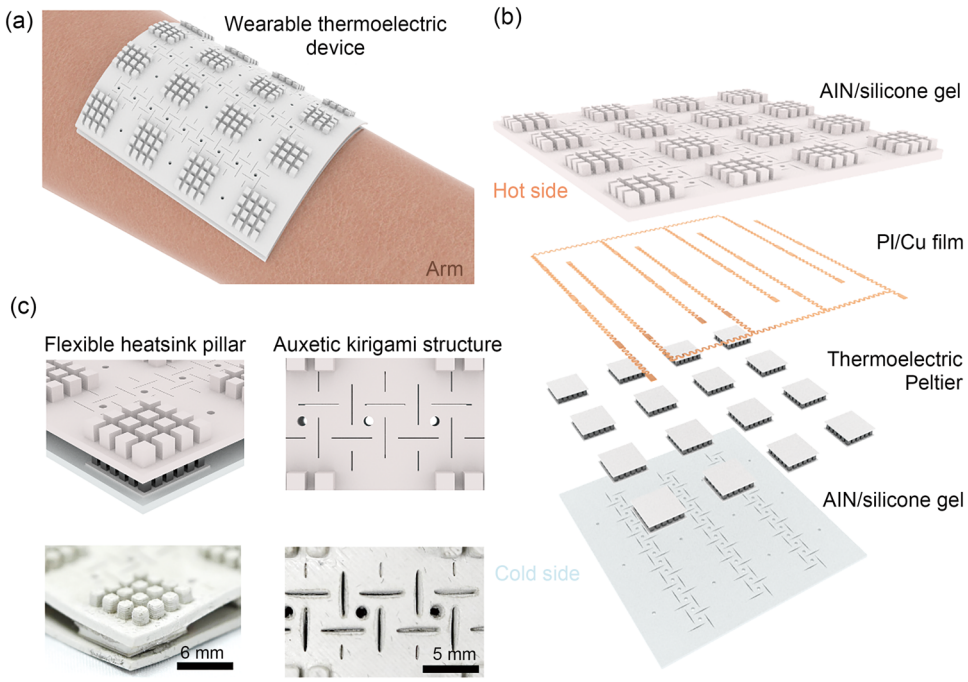

Fig. 1 Design details and fabrication of the wearable thermoelectric device (TED): **a** illustration of the application of the developed TED; **b** exploded views of the TED design; **c** illustration and photographs of the flexible heatsink pillar and auxetic kirigami structure. PI: polyimide

is illustrated in Fig. S4 (Supplementary Information). The deflection of silicone gels with the kirigami pattern under the same load is around 3.5 mm more than that of the sample without the pattern, thus demonstrating the exceptional flexibility of the structure (Figs. S5 and S6 in Supplementary Information). Figures 2i shows the effect of the kirigami structure on Poisson's ratio of the device. Owing to the auxetic effect of the kirigami structure, Poisson's ratio of the device decreased to 0.25. The simulation of the TED mechanical deformation under different strain rates is referenced in Fig. S7 (Supplementary Information). The auxetic effect of the kirigami structure can be explained by the rotational phenomenon of the square unit when strain is applied; details and characterizations are illustrated in Figs. S8 and S9 (Supplementary Information).

Characterizations

To improve the thermal conductivity of the stretchable silicone gel, AlN was added as the filler. AlN is an outstanding candidate for the filler in a thermal conductive stretchy gel in flexible electronic applications owing to its high thermal conductivity (up to 321 W/(m·K) [50]) and electrical insulation. In contrast with common thermal conductive fillers such as nano-silver wire, carbon nanotubes, or other metal particles, the usage of AlN does not necessitate an additional sealing layer to prevent short circuit. Figure 3a illustrates the thermal conductivity value of various ratios of AlN/silicone gel. The thermal conductivity increased from approximately 0.18 to 0.62 W/(m·K) by increasing the AlN mass fraction to 37.5%. The cross-sectional SEM images of AlN/silicone gel with different ratios are listed in Figs. S10 and S11 (Supplementary Information). The AlN powder can be evenly distributed in the silicone gel through the proposed fabrication method to ensure thermal conductivity. Although further increasing AlN content can improve the thermal conductivity of the gel, the viscosity of the uncured mixture is too high for molding, and the gel cannot cure completely when the AlN mass fraction is increased to 42%. Thus, we selected 37.5% (mass fraction) of AlN for further development. The rheological properties are listed in Fig. S12 (Supplementary Information) for reference. The developed AlN/silicone gel shows good adhesion (Fig. S13 in Supplementary Information) with the thermoelectric Peltier, which prevents detachment and ensures long-term performance during application. To highlight the robustness and flexibility of our design, we have conducted various experiments in terms of electrical resistance (Figs. 3b and 3c) under different curvatures and different numbers of bending cycles. The excellent stability of resistance further confirms the result of our finite element analysis. We simulated the cooling/heating effect of the device on human skin with the laboratory setup shown in Fig. S1 (Supplementary Information). We evaluated the temperature change of the fiber-type thermocouples inserted between the heater and device when −0.50–0.50 A of electricity is applied. The negative and positive values of the current input refer to the heating and cooling effects, respectively. The result suggests that the device was able to achieve around 3.8 and 3.5 °C heating and cooling effects

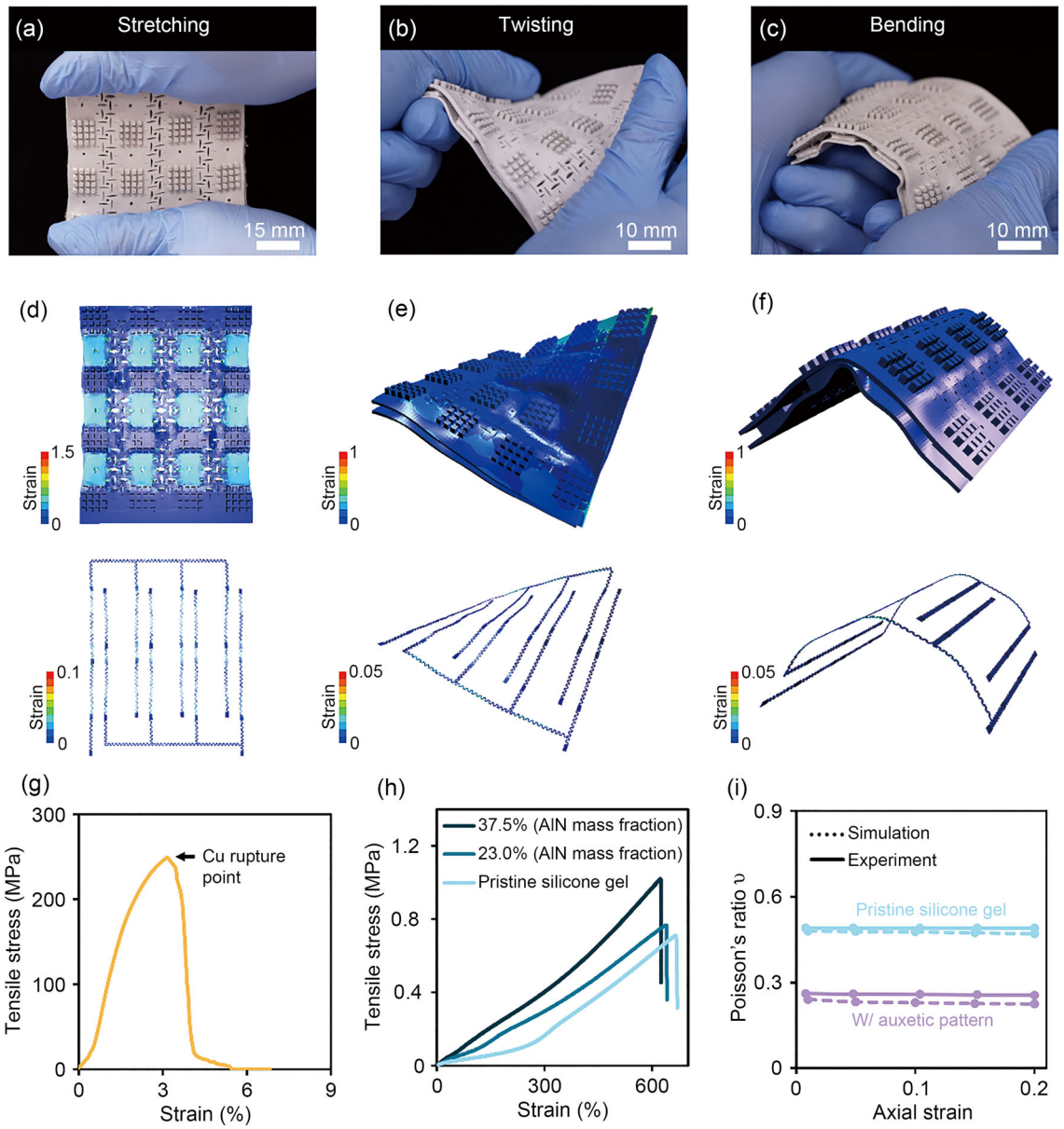

Fig. 2 Mechanical analysis of the thermoelectric device (TED): **a–c** photographs of the flexible TED under stretching (strain: 0.2), twisting (twist angle: 60°), and bending (bending radius: 30 mm); **d–f** strain distribution of the outermost silicone gel and inter-stretchable serpentine circuit based on the finite element analysis; **g** experiment on the stress–strain behavior of PI/Cu thin film; **h** experiment on the stress–strain behavior of AlN/silicone gel with different AlN ratios; **i** comparison between the experimental and simulation results of Poisson's ratio change under axial strain. W/: with

when −0.50 and 0.50 A of electricity were applied, respectively (Fig. 3d). Moreover, the temperature change under different applied current can remain unchanged under different curvatures, strains, and twists (Figs. 3e and 3f) that simulate the human body motion during the real application. As a wearable device, water vapor from our skin should be able to pass through the device to ensure comfortability, which was hardly investigated in previous wearable TED designs.

The accumulated perspiration that cannot be evaporated from the skin surface can cause redness, itchiness, and inflammation. With the developed kirigami pattern, our device can achieve a water vapor transmission rate of 4.9 kg/(m^2·d) (Fig. S14 in Supplementary Information). Instead of thermoregulation, the device can also be applied for power generation based on the temperature difference between both sides. The average Seeback coefficient (S) of our device was 0.470 mV/K (Fig. 3g). When the temperature

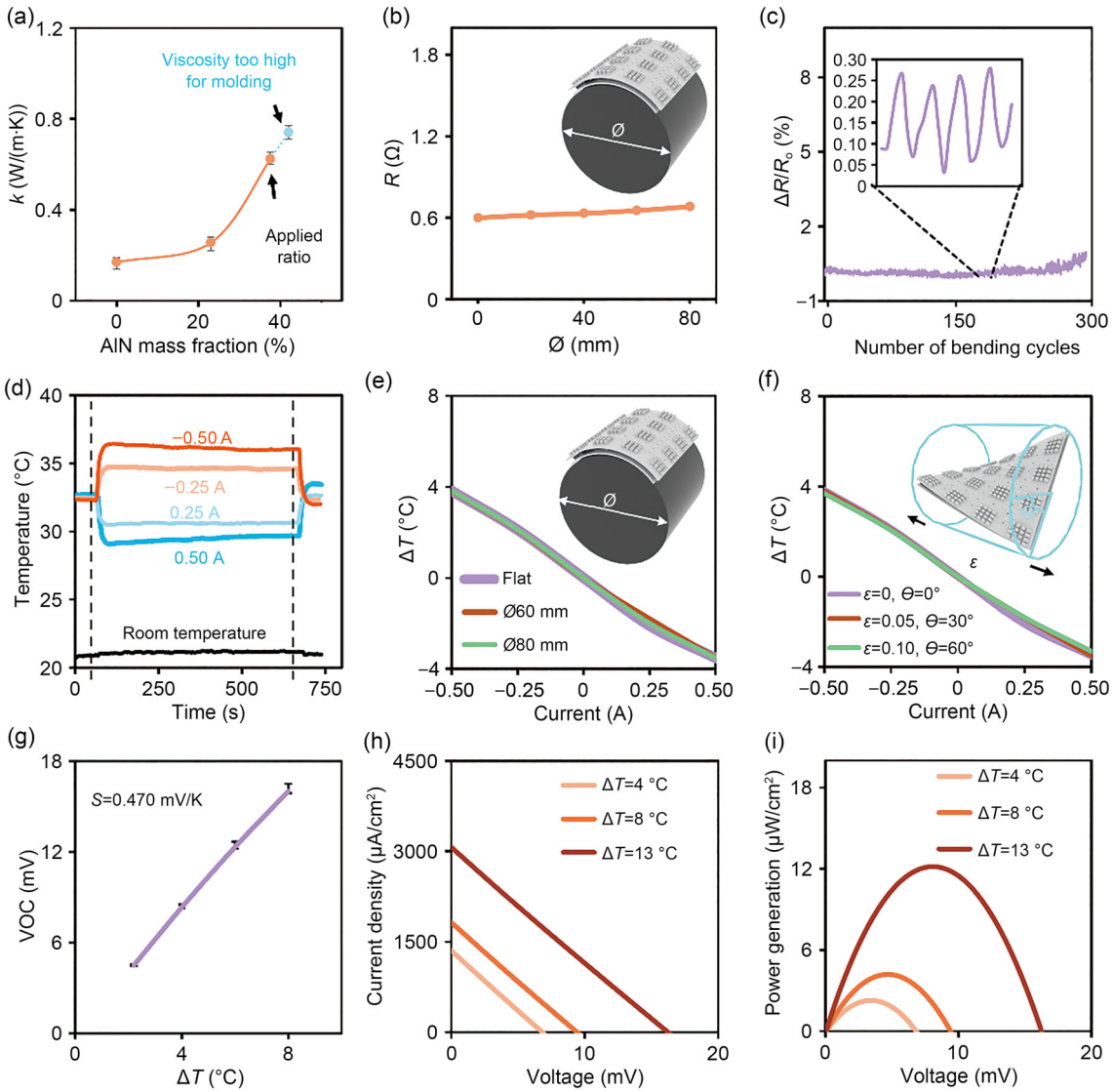

Fig. 3 Characterization of the developed thermoelectric device (TED): **a** thermal conductivity *k* of AlN/silicone gel with different AlN ratios; **b** electrical resistance of the TED under different curvatures; **c** electrical resistance change of the TED after 300 bending cycles; **d** effect of cooling or heating of the TED under different current inputs; **e** performance of the TED under different bending levels; **f** performance of the TED under different strains and twist angles simultaneously; **g** open-circuit voltages under the temperature difference of both sides; **h** current density and **i** power generation of the TED under different voltages at various temperature differences

difference is 13 °C, the maximum current and power generation could reach around 3070 μA/cm^2 and 12.2 μW/cm^2, respectively.

Wear trial

To demonstrate the ability of the developed TED for thermoregualtion of the human body, we conducted a trial. Figures 4a–4d show the photographs of the experimental setup, average skin temperature result, and the experiment protocol. For cooling, 0.50 A of electricity was applied, resulting in an average skin temperature drops of 3.5 °C. For heating, −0.25 A of electricity was applied, resulting in an average skin temperature increase by 1.7 °C. Figures 4e–4g show the infrared images taken after the removal of TED, demonstrating the cooling and heating effects provided by the TED. During the experiment, the subject reported that the cooling and heating effects provided by the TED could be perceived. Additionally, no discomfort or pain was reported by the subject. There may be a minor temperature variation overall owing to the uneven level of Joule heating effect caused by the variable electric current in the parallel circuit design and soldering flaws. It should be noted that wearable TEDs are not only limited to body thermoregulation applications; they are also applicable for wound care and thermal therapy for muscles or joints. In the early stages of wound

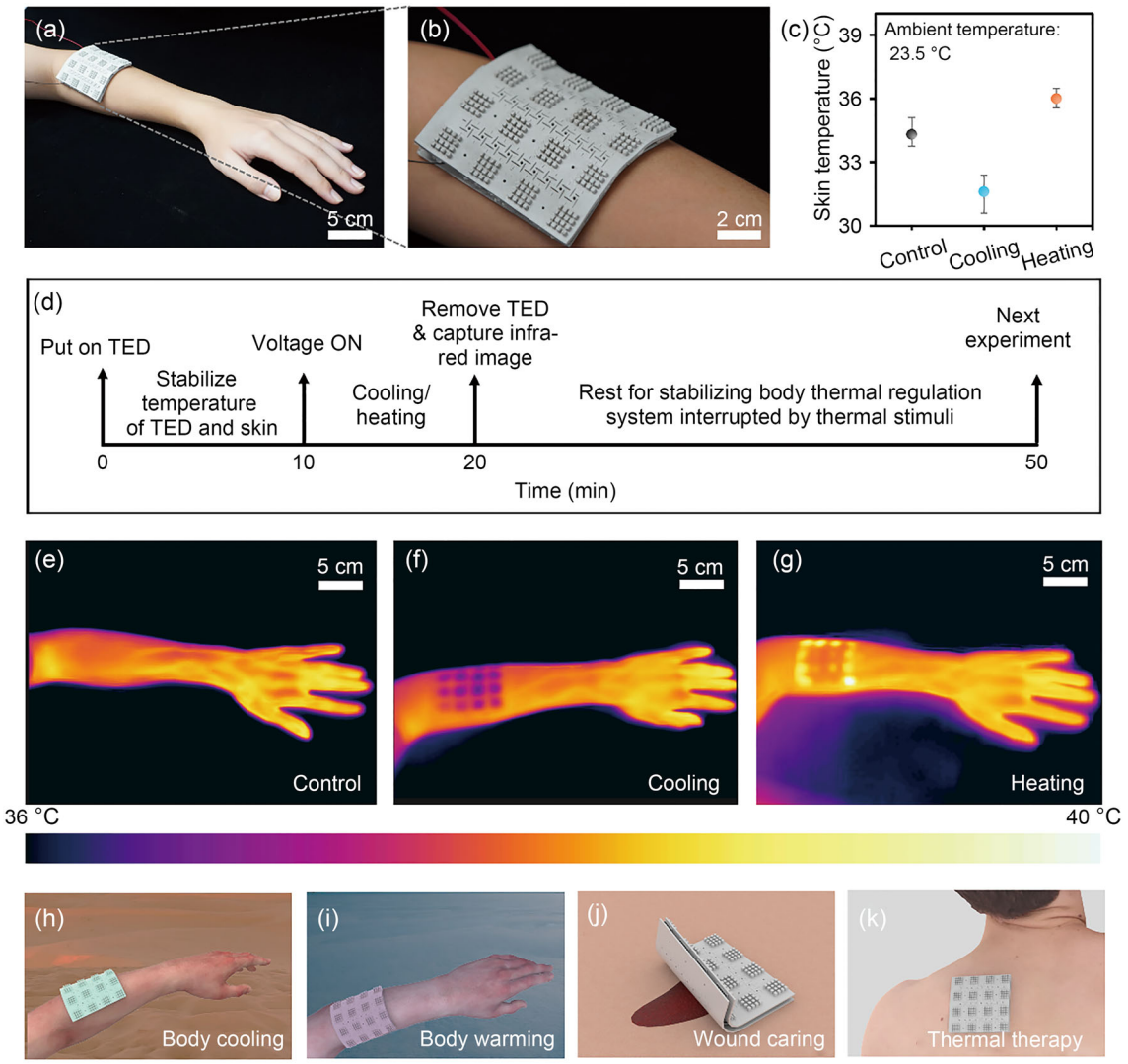

Fig. 4 Wear trial and demonstration of the developed thermoelectric device (TED): **a**, **b** photographs of the experimental setup and the close up of the TED; **c** effect of cooling (0.50 A) or heating (−0.25 A) provided by the TED (data are expressed as mean±standard deviation, n=3); **d** protocol of the wear trial; **e**–**g** thermal images showing the cooling and heating effects of the TED; **h**–**k** potential applications for the TED

healing, cold therapy (also known as cryotherapy) can be provided by the wearable TED to constrict the blood vessels, reducing the blood circulation and metabolic activity at the wound area, thus reducing the inflammation and pain level [51, 52]. Contrarily, it is recommended that raising the temperature at the wound area during the later phases of healing, or in the case of chronic wounds, to enhance blood flow will help provide essential nutrients and oxygen, thereby speeding the healing process [53, 54]. Exploiting the flexibility of the wearable TED that can provide heating and cooling effects not only saves time for applying abundant equipment, but also improves patients' compliance and precision for home wound caring programs. Moreover, the application of TEDs via thermal therapy is beneficial to muscles or joint stiffness. Conventional rigid wearable TEDs have been utilized to reduce shoulder stiffness [55]. The rigidity of TEDs has constrained the placement of the device in the therapeutic area. By introducing a facile technique that enhances device conformability, we expand the potential application of TEDs for thermal therapy. Figure S15 (Supplementary Information) illustrates the differences between the conventional rigid TED and soft TED for deltoid muscle and knee thermal therapy.

Conclusions

We introduced a body conformable, flexible, and stretchable kirigami-based wearable TED. The flexibility and conformability of TEDs were enhanced by utilizing a kirigami pattern

and stretchable circuits. The kirigami pattern created openings, allowing the wearable TED to exhibit good water vapor transmissibility (4.9 kg/(m^2·d)). The device can increase or decrease the skin temperature by 3.8 or 3.5 °C by applying −0.50 or 0.50 A of electricity, respectively. The finite element analysis result reveals the outstanding mechanical performance of the developed device, which can be operated normally under stretching (strain: 0.2), twisting (twist angle: 60°), and bending (bending radius: 30 mm). The wear trial demonstrates the feasibility of the thermal management of the kirigami-based design. The incorporation of kirigami patterns into wearable TEDs addresses the previous constraint, as their exceptional flexibility allows them to be applied to various uneven surfaces. Our demonstration can also provide new insight for developing flexible electronics that require a high degree of deformation.

Supplementary Information The online version contains supplementary material available at https://doi.org/10.1007/s42242-024-00290-6.

Acknowledgements This work was supported by the National Natural Science Foundation of China (No. 62122002), the Project of City University of Hong Kong (Nos. 9667221, 9678274, and 9680322), as part of the InnoHK Project on Project 2.2—AI-based 3D ultrasound imaging algorithm at Hong Kong Centre for Cerebro-Cardiovascular Health Engineering (COCHE), and the Project of Research Grants Council of the Hong Kong Special Administrative Region (Nos. 11213721, 11215722, and 11211523).

Author contributions XGY and LC initiated the concept and proposed the project. LC developed the device and collected the overall data. GYZ and LC led and developed the laser cutting process. PCW and LC carried out the mechanical modeling of circuit design and finite element analysis. XCH, JYL, JL (Jian Li), WYW, and GHG assisted in fabrication and characterization. ZYL, JCW, JKZ, YWY, and LC organized the wear trial. LC and XGY wrote the manuscript. All authors contributed to discussing the data and commenting on the final manuscript.

Declarations

Conflict of interest XGY is an associate editor for *Bio-Design and Manufacturing* and was not involved in the editorial review or the decision to publish this article. All the authors declare that they have no conflict of interest.

Ethical approval All experiments involving human subjects were approved by the Research Committee of City University of Hong Kong, China, and conducted in compliance with the guidelines. The participants were informed and provided with written consent before taking part in the study.

References

1. Li XQ, Guo WL, Hsu PC (2023) Personal thermoregulation by moisture-engineered materials. Adv Mater 2023:2209825. https://doi.org/10.1002/adma.202209825
2. Hong S, Gu Y, Seo JK (2019) Wearable thermoelectrics for personalized thermoregulation. Sci Adv 5(5):eaae0536. https://doi.org/10.1126/sciadv.aaw0536
3. Smallcombe JW, Foster J, Hodder SG (2022) Quantifying the impact of heat on human physical work capacity; part IV: interactions between work duration and heat stress severity. Int J Biometeorol 66:2463–2476. https://doi.org/10.1007/s00484-022-02370-7
4. Osilla EV, Marsidi JL, Shumway KR (2023) Physiology Temperature Regulation. StatPearls Publishing, Treasure Island, USA
5. Elsaid AM, Mohamed HA, Abdelaziz GB et al (2021) A critical review of heating, ventilation, and air conditioning (HVAC) systems within the context of a global SARS-CoV-2 epidemic. Process Safety Environ Protect 155:230–261. https://doi.org/10.1016/j.psep.2021.09.021
6. Shi XL, Zou J, Chen ZG (2020) Advanced thermoelectric design: from materials and structures to devices. Chem Rev 120:7399–7515. https://doi.org/10.1021/acs.chemrev.0c00026
7. Veselý M, Zeiler W (2014) Personalized conditioning and its impact on thermal comfort and energy performance—a review. Renew Sust Energy Rev 34:401–408. https://doi.org/10.1016/j.rser.2014.03.024
8. McLinden MO, Brown JS, Brignoli R et al (2017) Limited options for low-global-warming-potential refrigerants. Nat Commun 8:14476. https://doi.org/10.1038/ncomms14476
9. Heo SY, Lee GJ, Song YM (2022) Heat-shedding with photonic structures: radiative cooling and its potential. J Mater Chem C 10:9915–9937. https://doi.org/10.1039/D2TC00318J
10. Ernst TC, Garimella S (2013) Demonstration of a wearable cooling system for elevated ambient temperature duty personnel. Appl Therm Eng 60(1–2):316–324. https://doi.org/10.1016/j.applthermaleng.2013.06.019
11. Li JY, Fu Y, Zhou JK et al (2023) Ultrathin, soft, radiative cooling interfaces for advanced thermal management in skin electronics. Sci Adv 9(14):eadg1837. https://doi.org/10.1126/sciadv.adg1837
12. Wang HM, Zhang Y, Liang XP et al (2021) Smart fibers and textiles for personal health management. ACS Nano 15(8):12497–12508. https://doi.org/10.1021/acsnano.1c06230
13. Kang MH, Lee GJ, Lee JH et al (2021) Outdoor-useable, wireless/battery-free patch-type tissue oximeter with radiative cooling. Adv Sci 8(10):2004885. https://doi.org/10.1002/advs.202004885
14. Byun SH, Yun JH, Heo SY et al (2022) Self-cooling gallium-based transformative electronics with a radiative cooler for reliable stiffness tuning in outdoor use. Adv Sci 9(24):2202549. https://doi.org/10.1002/advs.202202549
15. Dou SL, Xu HB, Zhao JP et al (2021) Bioinspired microstructured materials for optical and thermal regulation. Adv Mater 33(6):2000697. https://doi.org/10.1002/adma.202000697
16. Savage N (2009) Thermoelectric coolers. Nat Photon 3:541–542. https://doi.org/10.1038/nphoton.2009.158
17. Minnich AJ, Dresselhaus MS, Ren ZF et al (2009) Bulk nanostructured thermoelectric materials: current research and future prospects. Energy Environ Sci 2(5):466–479. https://doi.org/10.1039/B822664B
18. Drebushchak VA (2008) The Peltier effect. J Therm Anal Calorim 91:311–315. https://doi.org/10.1007/s10973-007-8336-9
19. Zhang QH, Deng KF, Wilkens L et al (2022) Micro-thermoelectric devices. Nat Electron 5:333–347. https://doi.org/10.1038/s41928-022-00776-0
20. Cao TY, Shi XL, Chen ZG (2023) Advances in the design and assembly of flexible thermoelectric device. Prog Mater Sci 131:101003. https://doi.org/10.1016/j.pmatsci.2022.101003
21. Yang SQ, Qiu PF, Chen LD et al (2021) Recent developments in flexible thermoelectric devices. Small Sci 1(7):2100005. https://doi.org/10.1002/smsc.202100005
22. Kanahashi K, Pu J, Takenobu T (2020) 2D materials for large-area flexible thermoelectric devices. Adv Energy Mater 10(11):1902842. https://doi.org/10.1002/aenm.201902842

23. Wei HX, Zhang J, Han Y et al (2022) Soft-covered wearable thermoelectric device for body heat harvesting and on-skin cooling. Appl Energy 326:119941. https://doi.org/10.1016/j.apenergy.2022.119941
24. Liu Y, Zhuo FL, Zhou J et al (2022) Machine-learning assisted handwriting recognition using graphene oxide-based hydrogel. ACS Appl Mater Interfaces 14(18):54276–54286. https://doi.org/10.1021/acsami.2c17943
25. Yu SZ, Hou YC, Jin QJ et al (2023) Biomimetic chlorophyll derivatives-based photocatalytic fabric for highly efficient O_2 production via CO_2 and H_2O photoreaction. Chem Eng J 472:145103. https://doi.org/10.1016/j.cej.2023.145103
26. Bang KM, Park W, Ziolkowski P et al (2021) Fabrication and cooling performance optimization of stretchable thermoelectric cooling device. ACS Appl Electron Mater 3(12):5433–5442. https://doi.org/10.1021/acsaelm.1c00886
27. Choi J, Dun CC, Forsythe C et al (2021) Lightweight wearable thermoelectric cooler with rationally designed flexible heatsink consisting of phase-change material/graphite/silicone elastomer. J Mater Chem A 9(28):15696–15703. https://doi.org/10.1039/D1TA01911B
28. Zhang Y, Gao J, Zhu SJ et al (2022) Wearable thermoelectric cooler based on a two-layer hydrogel/nickel foam heatsink with two-axis flexibility. ACS Appl Mater Interfaces 14(13):15317–15323. https://doi.org/10.1021/acsami.2c01777
29. Sugahara T, Ekubaru Y, Nong NV et al (2019) Fabrication with semiconductor packaging technologies and characterization of a large-scale flexible thermoelectric module. Adv Mater Technol 4(2):1800556. https://doi.org/10.1002/admt.201800556
30. Yang Y, Hu HJ, Chen ZY et al (2020) Stretchable nanolayered thermoelectric energy harvester on complex and dynamic surfaces. Nano Lett 20(6):4445–4453. https://doi.org/10.1021/acs.nanolett.0c01225
31. Sato Y, Terashima S, Iwase E (2023) Origami-type flexible thermoelectric generator fabricated by self-folding. Micromachines 14(1):218. https://doi.org/10.3390/mi14010218
32. Rösch AG, Gall A, Aslan S et al (2021) Fully printed origami thermoelectric generators for energy-harvesting. npj Flex Electron 5:1. https://doi.org/10.1038/s41528-020-00098-1
33. Rafsanjani A, Bertoldi K (2017) Buckling-induced kirigami. Phys Rev Lett 118:084301. https://doi.org/10.1103/PhysRevLett.118.084301
34. Blees MK, Barnard AW, Rose PA et al (2015) Graphene kirigami. Nature 524:204–207. https://doi.org/10.1038/nature14588
35. Lamoureux A, Lee K, Shlian M et al (2015) Dynamic kirigami structures for integrated solar tracking. Nat Commun 6:8092. https://doi.org/10.1038/ncomms9092
36. Wu CS, Wang X, Lin L et al (2016) Paper-based triboelectric nanogenerators made of stretchable interlocking kirigami patterns. ACS Nano 10(4):4652–4659. https://doi.org/10.1021/acsnano.6b00949
37. Kim DH, Lu N, Ma R et al (2011) Epidermal electronics. Science 333(6044):838–843. https://doi.org/10.1126/science.1206157
38. Rogers JA, Someya T, Huang YG (2010) Materials and mechanics for stretchable electronics. Science 327(5973):1603–1607. https://doi.org/10.1126/science.1182383
39. Webb RC, Bonifas AP, Behnaz A et al (2013) Ultrathin conformal devices for precise and continuous thermal characterization of human skin. Nat Mater 12:938–944. https://doi.org/10.1038/nmat3755
40. Liu YH, Pharr M, Salvatore GA (2017) Lab-on-skin: a review of flexible and stretchable electronics for wearable health monitoring. ACS Nano 11(10):9614–9635. https://doi.org/10.1021/acsnano.7b04898
41. Brooks AK, Chakravarty S, Ali M et al (2022) Kirigami-inspired biodesign for applications in healthcare. Adv Mater 34(18):2109550. https://doi.org/10.1002/adma.202109550
42. Luo YF, Abidian MR, Ahn JH et al (2023) Technology roadmap for flexible sensors. ACS Nano 17:5211–5295. https://doi.org/10.1021/acsnano.2c12606
43. Davoodi E, Montazerian H, Khademhosseini A et al (2020) Sacrificial 3D printing of shrinkable silicone elastomers for enhanced feature resolution in flexible tissue scaffolds. Acta Biomater 117:261–272. https://doi.org/10.1016/j.actbio.2020.10.001
44. ASTMD5169-98 (2021) Standard test method for shear strength (dynamic method) of hook and loop touch fastener. ASTM International, West Conshohocken. https://doi.org/10.1520/D5169-98R21
45. Yang WZ, Gao ZZ, Yue ZF et al (2019) Hard-particle rotation enabled soft–hard integrated auxetic mechanical metamaterials. Proc Royal Soc A Math Phys Eng Sci 475(2228):20190234. https://doi.org/10.1098/rspa.2019.0234
46. Chow L, Yick KL, Wong KH et al (2022) 3D printing auxetic architectures for hypertrophic scar therapy. Macromol Mater Eng 307(5):2100866. https://doi.org/10.1002/mame.202100866
47. Corrigan T, Fleming P, Eldredge C et al (2023) Strong conformable structure via tension activated kirigami. Commun Mater 4:31. https://doi.org/10.1038/s43246-023-00357-4
48. Cho H, Seo D, Kim DN (2018) Mechanics of auxetic materials. In: Hsueh CH, Schmauder S, Chen CS et al (Eds.), Handbook of Mechanics of Materials. Springer, Singapore, p.733–757. https://doi.org/10.1007/978-981-10-6884-3_25
49. Chen J, Jiang JH, Weber J et al (2023) Shape morphing by topological patterns and profiles in laser-cut liquid crystal elastomer kirigami. ACS Appl Mater Interfaces 15(3):4538–4548. https://doi.org/10.1021/acsami.2c20295
50. Cheng Z, Koh YR, Mamun A et al (2020) Experimental observation of high intrinsic thermal conductivity of AlN. Phys Rev Mater 4:044602. https://doi.org/10.1103/PhysRevMaterials.4.044602
51. Kwiecien SY, McHugh MP (2021) The cold truth: the role of cryotherapy in the treatment of injury and recovery from exercise. Eur J Appl Physiol 121:2125–2142. https://doi.org/10.1007/s00421-021-04683-8
52. John SS, Mohanty S, Chaudhary Z et al (2020) Comparative evaluation of low level laser therapy and cryotherapy in pain control and wound healing following orthodontic tooth extraction: a double blind study. J Cranio-Maxillofacial Surg 48(3):251–260. https://doi.org/10.1016/j.jcms.2020.01.012
53. Yang X, He SS, Wang J et al (2023) Hyaluronic acid-based injectable nanocomposite hydrogels with photo-thermal antibacterial properties for infected chronic diabetic wound healing. Int J Biol Macromol 242:124872. https://doi.org/10.1016/j.ijbiomac.2023.124872
54. Freedman BR, Hwang C, Talbot S et al (2023) Breakthrough treatments for accelerated wound healing. Sci Adv 9:eade7007. https://doi.org/10.1126/sciadv.ade7007
55. Sawada T, Okawara H, Nakashima D et al (2022) Effects of alternating heat and cold stimulation using a wearable thermo-device on subjective and objective shoulder stiffness. J Physiol Anthropol 41:1. https://doi.org/10.1186/s40101-021-00275-9